

2009

Adiabatically induced coherent Josephson oscillations of ultracold atoms in an asymmetric two-dimensional magnetic lattice

Ahmed Abdelrahman
Edith Cowan University

Peter Hannaford

Kamal Alameh
Edith Cowan University

Follow this and additional works at: <https://ro.ecu.edu.au/ecuworks>



Part of the [Engineering Commons](#)

This paper was published in Optics Express and is made available as an electronic reprint with the permission of OSA. The paper can be found at the following URL on the OSA website: <http://www.opticsinfobase.org/abstract.cfm?URI=oe-17-26-24358>. Systematic or multiple reproduction or distribution to multiple locations via electronic or other means is prohibited and is subject to penalties under law.

This Journal Article is posted at Research Online.

<https://ro.ecu.edu.au/ecuworks/459>

Adiabatically induced coherent Josephson oscillations of ultracold atoms in an asymmetric two-dimensional magnetic lattice

A. Abdelrahman^{1*}, P. Hannaford² and K. Alameh¹

¹*Electron Science Research Institute, Edith Cowan University
270 Joondalup Drive, Perth WA 6027 Australia*

²*Centre for Atom Optics and Ultrafast Spectroscopy, and ARC Center of Excellence for
Quantum Atom Optics, Swinburne University of Technology, Melbourne, Australia 3122*

[*a.abdelrahman@ecu.edu.au](mailto:a.abdelrahman@ecu.edu.au)

Abstract: We propose a new method to create an asymmetric two-dimensional magnetic lattice which exhibits magnetic band gap structure similar to semiconductor devices. The quantum device is assumed to host bound states of collective excitations formed in a magnetically trapped quantum degenerate gas of ultracold atoms such as a Bose-Einstein condensate (BEC) or a degenerate Fermi gas. A theoretical framework is established to describe possible realization of the exciton-Mott to discharging Josephson states oscillations in which the adiabatically controlled oscillations induce *ac* and *dc* Josephson atomic currents where this effect can be used to transfer *n* Josephson qubits across the asymmetric two-dimensional magnetic lattice. We consider second-quantized Hamiltonians to describe the Mott insulator state and the coherence of multiple tunneling between adjacent magnetic lattice sites where we derive the self consistent non-linear Schrödinger equation with a proper field operator to describe the exciton Mott quantum phase transition via the induced Josephson atomic current across the *n* magnetic bands.

© 2009 Optical Society of America

OCIS codes: (020.1475) Bose-Einstein condensates; (270.5585) Quantum information and processing.

References and links

1. L. Perakis, "Condensed-matter physics: Exciton developments," *Nature* **33**, 417 (2002).
2. A. Abdelrahman, P. Hannaford, M. Vasiliev, and K. Alameh, "Asymmetric Two-dimensional Magnetic Lattices for Ultracold Atoms Trapping and Confinement," in progress, arXiv:0910.5032v1 [quant-ph] (2009).
3. L. V. Butov, A. C. Gossard, and D. S. Chemla, "Towards Bose-Einstein condensation of excitons in potential traps," *Nature* **47**, 417 (2002).
4. S. Ghanbari, T. D. Kieu, A. Sidorov, and P. Hannaford, "Permanent magnetic lattices for ultracold atoms and quantum degenerate gases," *J. Phys. B* **39**, 847 (2006).
5. B.V. Hall, S. Whitlock, F. Scharnberg, P. Hannaford, and A. Sidorov, "A permanent magnetic film atom chip for Bose-Einstein condensation," *J. Phys. B: At. Mol. Opt. Phys.* **39**, 27 (2006).
6. M. Singh, M. Volk, A. Akulshin, A. Sidorov, R. McLean, and P. Hannaford, "One dimensional lattice of permanent magnetic microtraps for ultracold atoms on an atom chip," *J. Phys. B: At. Mol. Opt. Phys.* **41**, 065301 (2008).
7. S. Ghanbari, T. D. Kieu, and P. Hannaford, "A class of permanent magnetic lattices for ultracold atoms," *J. Phys. B: At. Mol. Opt. Phys.* **40**, 1283 (2007).

8. V. S. Shchesnovich and V. V. Konotop, "Nonlinear tunneling of Bose-Einstein condensates in an optical lattice: Signatures of quantum collapse and revival," *Phys. Rev. A* **75**, 063628 (2007).
9. Y. Shin, G.-B. Jo, M. Saba, T. A. Pasquini, W. Ketterle, and D. E. Pritchard, "Optical weak link between two spatially separated Bose-Einstein condensates," *Phys. Rev. Lett.* **95**, 170402 (2005).
10. M. Albiez, R. Gati, J. Fölling, S. Hunsmann, M. Cristiani, and M. K. Oberthaler, "Direct observation of tunneling and nonlinear self-trapping in a single Bosonic Josephson junction," *Phys. Rev. Lett.* **95**, 010402 (2005).
11. M. Rigol, V. Rousseau, R. T. Scalettar, and R. R. P. Singh, "Collective Oscillations of Strongly Correlated One-Dimensional Bosons on a Lattice," *Phys. Rev. Lett.* **95**, 110402 (2005).
12. M. Holthaus and S. Stenholm, "Coherent control of the self-trapping transition," *Eur. Phys. J. B* **20**, 451 (2001).
13. B. J. Dalton, "Two-mode theory of BEC interferometry," *J. Mod. Opt.* **54**, 615 (2007).
14. D. R. Dounas-Frazer and L. D. Carr, "Tunneling resonances and entanglement dynamics of cold bosons in the double well," *quant-ph/0610166* (2006).
15. S. Fölling, S. Trotzky, P. Cheinet, M. Feld, R. Saers, A. Widera, T. Müller, and I. Bloch, "Direct observation of second-order atom tunnelling," *Nature* **448**, 1029 (2007).
16. A. Smerzi, S. Fantoni, S. Giovanazzi, and S. R. Shenoy, "Quantum coherent atomic tunneling between two Trapped Bose-Einstein condensates," *Phys. Rev. Lett.* **79**, 4950 (1997).
17. J. Javanainen, "Oscillatory exchange of atoms between traps containing Bose condensates," *Phys. Rev. Lett.* **57**, 3164 (1986).
18. A. Smerzi, A. Trombettoni, T. Lopez-Arias, C. Fort, P. Maddaloni, F. Minardi, and M. Inguscio, "Macroscopic oscillations between two weakly coupled Bose-Einstein condensates," *Eur. Phys. J. B* **31**, 457 (2003).
19. G. J. Milburn and J. Corney, "Quantum dynamics of an atomic Bose-Einstein condensate in a double-well potential," *Phys. Rev. Lett.* **55**, 4318 (1997).
20. M. Anderlini, P. J. Lee, B. L. Brown, J. Sebby-Strabley, William D. Phillips, and J. V. Porto, "Controlled exchange interaction between pairs of neutral atoms in an optical lattice," *Nature* **448**, 452 (2007).
21. J. Stenger, S. Inouye, D. M. Stamper-Kurn, H.-J. Miesner, A. P. Chikkatur, and W. Ketterle, "Spin domains in ground state spinor Bose-Einstein condensates," *Nature* **396**, 345 (1998).
22. W. Zhang, S. Yi, and L. You, "Bose-Einstein condensation of trapped interacting spin-1 atoms," *Phys. Rev. A* **70**, 043611 (2004).
23. S. Whitlock, R. Gerritsma, T. Fernholz, and R. J. C. Spreeuw, "Two-dimensional array of microtraps with atomic shift register on a chip," *New J. Phys.* **11**, 023021 (2009).
24. H. Zoubi and H. Ritsch, "Bright and dark excitons in an atom-pairfilled optical lattice within a cavity," *EPL* **82**, 14001 (2008).
25. H. Zoubi and H. Ritsch, "Excitons and cavity polaritons for cold-atoms in an optical lattice," in *Conference on Lasers and Electro-Optics/Quantum Electronics and Laser Science Conference and Photonic Applications Systems Technologies*, OSA Technical Digest (CD) (Optical Society of America, 2008), paper QThE3.
26. A. Abdelrahman, M. Vasiliev, K. Alameh, P. Hannaford, Yong-Tak Lee, and Byoung S. Ham, "Towards Bose-Einstein condensation of excitons in an asymmetric multi-quantum state magnetic lattice," *Numerical Simulation of Optoelectronic Devices (NUSOD)* (2009).
27. S. Ghanbari, P. B. Blakie, P. Hannaford, and T. D. Kien, "Superfluid to Mott insulator quantum phase transition in a 2D permanent magnetic lattice," *Eur. Phys. J. B* **70**, 305 (2009).
28. J. Williams, R. Walser, J. Cooper, E. Cornell, and M. Holland, "Nonlinear Josephson-type oscillations of a driven, two-component Bose-Einstein condensate," *Phys. Rev. A* **59**, R31 (1999).
29. S. Raghavan, A. Smerzi, S. Fantoni, and S. R. Shenoy, "Coherent oscillations between two weakly coupled Bose-Einstein condensates: Josephson effects, π oscillations, and macroscopic quantum self-trapping," *Phys. Rev. A* **59**, 620 (1999).
30. G. K. Brennen, C. M. Caves, P. S. Jessen, and I. H. Deutsch, "Quantum logic gates in optical lattices," *Phys. Rev. Lett.* **82**, 1060 (1999).
31. B. D. Josephson, "Tunneling Into Superconductors," *Phys. Lett.* **1**, 251 (1962).
32. S. Shapiro, "Josephson Currents in Superconducting Tunneling: The Effect of Microwaves and Other Observations," *Phys. Rev. Lett.* **11**, 80 (1963).
33. S. Giovanazzi, A. Smerzi, and S. Fantoni, "Josephson effects in dilute Bose-Einstein condensates," *Phys. Rev. Lett.* **84**, 4521 (2000).
34. S. Ashhab and Carlos Lobo, "External Josephson effect in Bose-Einstein condensates with a spin degree of freedom," *Phys. Rev. A* **66**, 013609 (2002).
35. F. S. Cataliotti, S. Burger, C. Fort, P. Maddaloni, F. Minardi, A. Trombettoni, A. Smerzi, and M. Inguscio, "Josephson junction arrays with Bose-Einstein condensates," *Science* **293**, 843 (2001).
36. B. Juliá-Díaz, M. Guilleumas, M. Lewenstein, A. Polls, and A. Sanpera, "Josephson oscillations in binary mixtures of $F=1$ spinor Bose-Einstein condensates," *Phys. Rev. A* **80**, 023616 (2009).
37. R. Gati, M. Albiez, J. Fölling, B. Hemmerling, and M. K. Oberthaler, "Realization of a single Josephson junction for Bose-Einstein condensates," *Appl. Phys. B* **82**, 207 (2006).
38. B. P. Anderson and M. A. Kasevich, "Macroscopic quantum interference from atomic tunnel arrays," *Science* **282**, 1686 (1998).

1. Introduction

Recently, magnetic lattices have been created using permanent magnetic materials fabricated with specific patterns to create periodically distributed non-zero magnetic local minima in one and two-dimensional configurations [2, 4]. Ultracold atoms and Bose-Einstein condensates (BECs) prepared in so-called low magnetic field seeking-states, can be trapped in such periodically distributed magnetic local minima to create the magnetic lattices configurations [6, 23]. The magnetic lattices are recognized as quantum devices with abilities to coherently access and manipulate the quantum states of the trapped ultracold atoms in a similar scenario to optical lattices [30].

These advances in the field of ultracold atoms open the way to study many interesting fundamental problems in different area of physics such as condensed matter [27] and quantum information processing [30]. Magnetic lattices created by trapping ultracold atoms are used to simulate such environments and critical quantum phase transitions because they can provide adiabatic control over interesting quantum phenomena such as quantum tunneling, superfluidity and formation of bound states of long lived quasi-particles, e.g., exciton BECs [24, 25]. Bound states are naturally hard to detect and it is difficult to access their individual quantum states due to the short lifetime and their fragile coupling to a desirable environment [1, 3].

One of the interesting problems is to detect and manipulate the phase coherence signature in a macroscopic quantum system. A well known example of the direct manifestation of a macroscopic phase coherence is the Josephson effect between two superfluids or two superconductors [31, 32]. Theoretically, the use of trapped ultracold atoms in varying periodically distributed potential fields has been proposed to simulate the Josephson effect [29, 33, 34, 36] and experimentally has been realized [35, 37, 38].

In this article we propose a new approach to create an asymmetric two-dimensional magnetic lattice which allows the trapped ultracold atoms to simulate collective excitations similar to those formed in condensed matter systems. The ultracold atoms can be trapped to maintain an asymmetric two-dimensional lattice configuration in which our proposed method offers the possibility of having a magnetic band gap structure. We also show the possibility of using this type of 2D magnetic lattice to simulate the adiabatically controlled oscillations of collective excitations such as the discharging Josephson states and the exciton-Mott quantum phase transition formed by coherent tunneling of cold atoms across the lattice's sites. In Section 2 we describe the method we use to create our asymmetrical magnetic lattice; in Section 3 we describe the tunneling mechanisms; and in Section 4 we establish a theoretical framework to describe the adiabatically induced atomic Josephson currents and the exciton-Mott phase transition using trapped ultracold atoms in the asymmetrical magnetic lattice.

2. The Asymmetric Two-Dimensional Magnetic Lattice

Magnetic lattices are realized by periodically distributing magnetic field minima across the surface of a permanent magnetic material. The distributed field minima follow the lattices patterns in which they are specifically engineered so that the magnetic minima are located in a free space at an effective working distance, d_{min} , from the surface. Depending on the fabricated patterns, the dimension of the periodicity can be selected, where one and two-dimensional magnetic lattices have been achieved and produced by trapping ultracold atoms using patterned permanent magnetic materials [6, 23].

We have developed a new method to create a two-dimensional magnetic lattice which allows symmetrical and asymmetrical configurations of the distributed magnetic field minima. To realize a two-dimensional magnetic lattice square-hole matrices are patterned on a surface of a magneto-optic film of thickness τ_{bim} by milling an $m \times m$ array of blocks such that each block is an array of $n \times n$ square holes, where n represents the number of holes of width α_h and

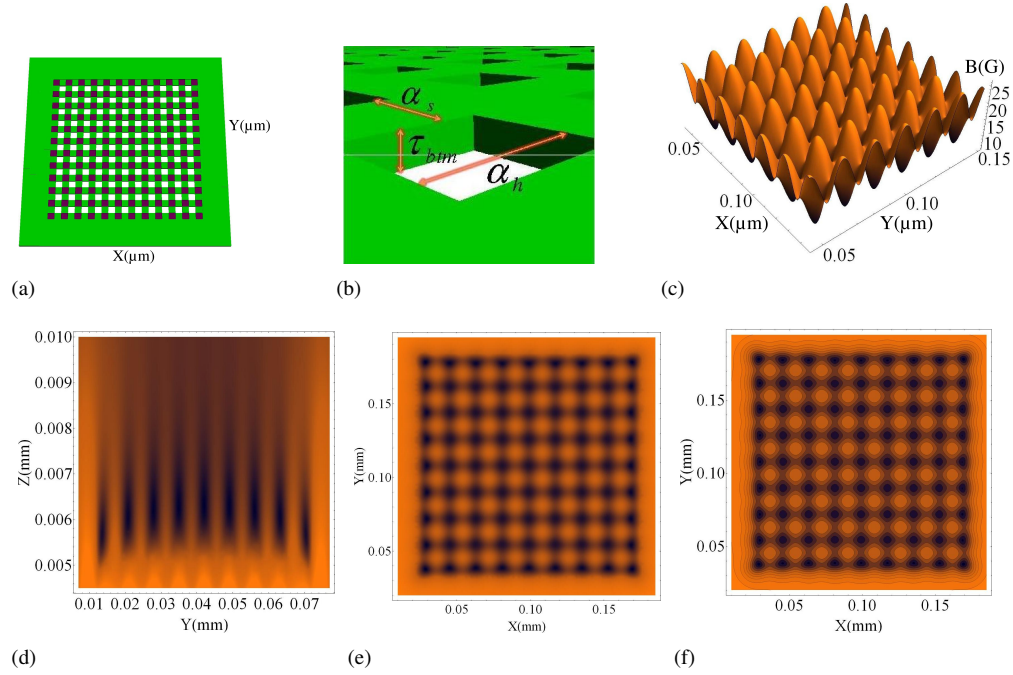


Fig. 1. (a) Schematic diagram of an 11×11 magnetic lattice surrounded by an unperturbed area. (b) The lattice parameters are specified by the hole size $\alpha_h \times \alpha_h$, the spacing α_s between the holes and the magnetic layer thickness τ_{btm} . (c) 3D plot of the magnetic field (along the z -axis) of the distributed sites across the $x-y$ plane simulated at a distance d_{min} from the surface. (d) Magnetic density plot of the simulated magnetic lattice sites in the $z-x$ plane along the center of the lattice. The traps (dark color) are located at the effective z -distance, d_{min} , from the surface of the magnetic film (bright color). (e-f) Magnetic field density and contour plots across the $x-y$ plane at d_{min} with no external magnetic bias fields, respectively. Simulation input parameters: $\alpha_s = \alpha_h = 7 \mu m$, $M_z = 2.80$ kG, $\tau_{btm} = 2 \mu m$ and $\tau_{p-wall} = 2 \mu m$.

separated by α_s within each block as shown in Figs. 1(a), 1(b). The depths of all holes are equal and extend through the magnetic thin film down to the substrate surface level. The magnetic structure is magnetized in its remanently-magnetized state, with the magnetization direction perpendicular to the $x-y$ plane. The gaps between the blocks containing no holes are assumed to be greater than, or equal to α_s . The thickness of the gaps is an important design feature since it introduces a control over an extra degree of confinement which is realized through the creation of magnetic field walls encircling the $n \times n$ matrices, and isolating them from one another. It also can control the magnetic bottom, B_{min} , and the distance from the surface, d_{min} , of the sites at the center of the magnetic lattice.

The presence of the holes on the surface of the permanent magnetic thin film results in a magnetic field with a maximum at the opening of the holes decreasing steeply outwards from the surface in the z direction and creating magnetic field minima that are located at effective working distances, d_{min} , above the plane of the thin film as shown in Figs. 1(d)–1(f). These minima are localized in confining volumes representing the magnetic potential wells that contain a certain number of quantized energy levels occupied by the ultracold atoms. In our design, we assumed that the width of the holes α_h and the separation of the holes α_s are equal,

$\alpha_h = \alpha_s \equiv \alpha$, to simplify the mathematical derivations and analyses which are similar to those reported in [4, 7].

2.1. Detailed Analysis of the Distribution of the Magnetic Field Minima

The spatial magnetic field components B_x , B_y and B_z can be written analytically as a combination of a field decaying away from the surface of the trap in the z -direction and a periodically distributed magnetic field in the $x-y$ plane produced by the magnetic induction, $B_o = \mu_o M_z / \pi$, at the surface of the permanently magnetized thin film. We define a surface reference magnetic field as $B_{ref} = B_o(1 - e^{-\beta\tau})$, where $\beta = \pi/\alpha$, and $\tau = \tau_{btm}$ denotes the magnetic film thickness and a plane of symmetry is assumed at $z = 0$. The analysis of the surface magnetic field includes components of external magnetic bias fields along the x , y and z directions, B_{x-bias} , B_{y-bias} and B_{z-bias} , respectively. Taking into account the surface effective field, B_{ref} , and the characteristic periodicity interval α , analytical expressions can be derived to describe the periodically distributed local minima across the $x-y$ plane of the magnetic thin film for the case of an infinite magnetic lattice as follows

$$B_x = B_{ref} \sin(\beta x) e^{-\beta[z-\tau]} - \frac{B_{ref}}{3} \sin(3\beta x) e^{-3\beta[z-\tau]} + \dots + B_{x-bias} \quad (1)$$

$$B_y = B_{ref} \sin(\beta y) e^{-\beta[z-\tau]} - \frac{B_{ref}}{3} \sin(3\beta y) e^{-3\beta[z-\tau]} + \dots + B_{y-bias} \quad (2)$$

$$B_z = B_{ref} [\cos(\beta x) + \cos(\beta y)] e^{-\beta[z-\tau]} - \frac{B_{ref}}{3} [\cos(3\beta x) + \cos(3\beta y)] e^{-3\beta[z-\tau]} + \dots + B_{z-bias} \quad (3)$$

Only cold atoms prepared in low magnetic field seeking states, i.e. atom's magnetic moment oriented anti-parallel to the local magnetic field in the trap, are attracted to the local magnetic minima, where at certain values of the effective distance d_{min} , namely larger than $\alpha/2\pi$, the cold atoms effectively interact with the local magnetic minima are loaded into the lattice sites. Thus the higher order terms in these equations can be neglected for $d_{min} > \alpha/2\pi$ reducing Eqs. (1),(2),(3) to the following simplified set of expressions

$$B_x = B_o \left(1 - e^{-\beta\tau}\right) e^{-\beta[z-\tau]} \times \sin(\beta x) + B_{x-bias} \quad (4)$$

$$B_y = B_o \left(1 - e^{-\beta\tau}\right) e^{-\beta[z-\tau]} \times \sin(\beta y) + B_{y-bias} \quad (5)$$

$$B_z = B_o \left(1 - e^{-\beta\tau}\right) e^{-\beta[z-\tau]} \times [\cos(\beta x) + \cos(\beta y)] + B_{z-bias} \quad (6)$$

Hence the magnitude B of the magnetic field at d_{min} above the surface of the magnetic film can be written as

$$B = \left\{ B_{x-bias}^2 + B_{y-bias}^2 + B_{z-bias}^2 + 2B_{ref}^2 \left[1 + \cos(\beta x) \cos(\beta y) \right] e^{-2\beta[z-\tau]} + 2B_{ref} \times \right. \\ \left. \times e^{-\beta[z-\tau]} \left(\sin(\beta x) B_{x-bias} + \sin(\beta y) B_{y-bias} + [\cos(\beta x) + \cos(\beta y)] B_{z-bias} \right) \right\}^{1/2} \quad (7)$$

A detailed analysis of the effect of the characteristic parameters, such as α_s , α_h , is reported elsewhere [2].

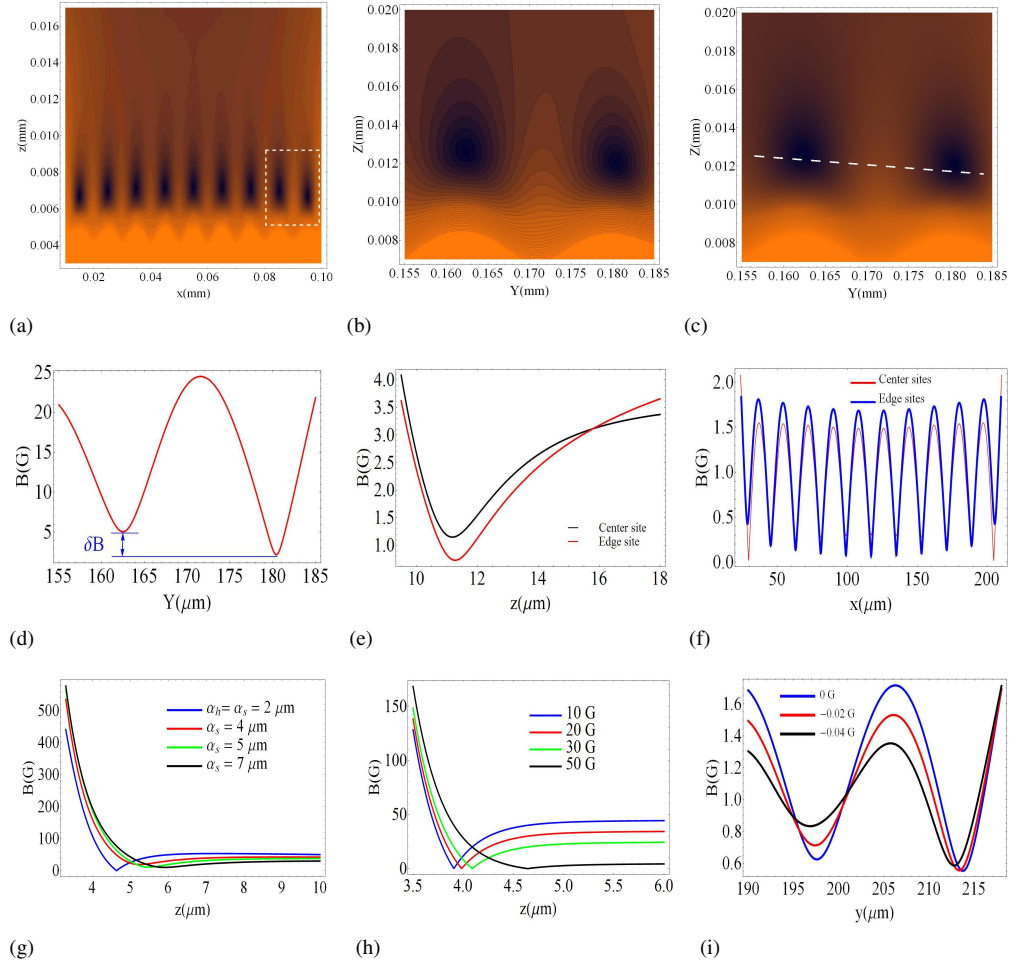


Fig. 2. (a) Magnetic field density plot of the simulation of a 9×9 magnetic lattice where the magnetic local minima are located at d_{min} above the holes. The central sites of the lattice exhibit larger distances from the magnetic thin film surface than the edge sites. (b-d) Contour and magnetic field density plots of two adjacent edge sites showing the separating distance along the gravitational field z -axis and the magnetic potential tilt, δB , and the magnetic tunneling barriers, ΔB , between the two sites. The magnetic field is calculated across the two sites as indicated by the dashed line. (e) Comparison of the magnetic field local minima along the z -axis at the center and the edge sites. (f) Two different magnetic bands at the center and at the edge of the asymmetrical magnetic lattice. (g) Simulated B_{min}^z for different values of α_s where the width of the holes is fixed, $\alpha_h = 2 \mu m$. (h) The effect of applying a varying external magnetic bias field on the non-zero local minima along the z -axis. (i) Tunneling barriers can adiabatically be controlled via applying the magnetic bias field B_{z-bias} along the z -axis. Simulation results show the effect of B_{z-bias} on ΔB and δB . Simulation inputs: $\alpha_s = \alpha_h = 7 \mu m$, $M_z = 2.80$ kG, $\tau_{btm} = 2 \mu m$ and $\tau_{n-wall} = -0.5 \mu m$.

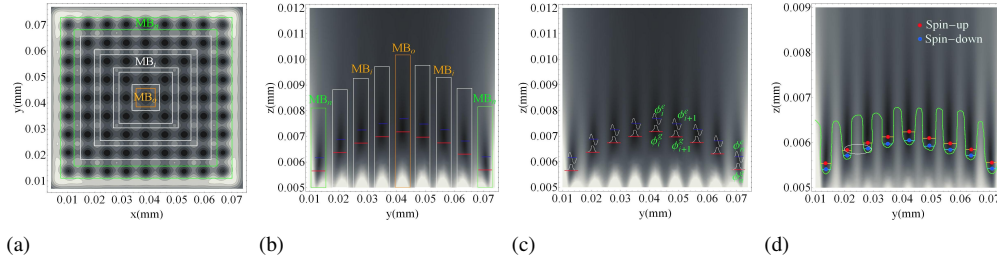


Fig. 3. (a-b) Schematic representation of the magnetic band structure (the pyramid-like distribution) where each band contains a set of magnetic minima. (c-d) Schematic representation of the two-modes configuration and a possible scenario of coupled spins between two magnetic bands hosting two different degrees of freedom of spins such a two-components spinor BECs or ultracold Fermions.

2.2. Magnetic Band Structure in the Asymmetric Two-Dimensional Magnetic Lattice

The asymmetric property of the two-dimensional magnetic lattice is created due to the existence of different levels of the non-zero magnetic local minima in a finite magnetic lattice. As shown in Fig. 2, each neighboring magnetic quantum wells, i.e., lattice sites, are separated by a tunneling barrier ΔB and their magnetic bottoms are displaced in the gravitational field z -direction by a titling potential δB . Both ΔB and δB can be controlled by applying an external magnetic bias field along the negative direction of the z -axis, as shown in Fig. 2(i).

The sites in the center of the magnetic lattice exhibit the deepest magnetic minima, where the values of the magnetic minima, B_{min} , are distributed in space downward to the edges of the lattice, see Fig. 2(f). The distribution has a pyramid shape in the $x - y$ plane where each level has its B_{min}^z value and the values of the B_{min} are spaced along the z -axis by a tilting potential δB . The potential tilt creates a gap between each two sets of magnetic minima distributed in two adjacent bands. This configuration exhibits a scenario similar to that of the energy band gap structure in semiconductor devices. We denote the pyramid-like distribution by a magnetic band gap structure in our proposed two-dimensional magnetic lattice. A schematic representation for the pyramid-like distribution is shown in Fig. 3.

Initially, with no application of external magnetic bias fields, B_{x-bias} and B_{y-bias} , all sites have magnetic minima close to zero. Once the external magnetic bias field is applied the values of the magnetic minima increase and differ from neighboring sites by the titling magnetic potential δB as shown in Fig. 2(d). The amount of tilt δB can be calculated from

$$\delta B = B_{min}^{i,l} - B_{min}^{i+1,l+1} \quad (8)$$

where $i = 0, 1, 2, \dots, n$ is the non-zero local minimum index at each band represented by $l = 0, 1, 2, \dots, N$ assuming there are N magnetic bands starting from the center of the lattice. The magnetic band gap is given by the difference between the maximum of the tunneling barrier, B_{max} , and the magnetic bottom of the lattice site, B_{min} , and is denoted by the tunneling barrier height

$$\Delta B = B_{max}^{i,l} - B_{min}^{i,l} \quad (9)$$

The non-zero local minimum values determine the depth Λ_{depth} of the harmonic potential wells in which Λ_{depth} of an individual potential well can be expressed as

$$\Lambda_{depth}(r) = \frac{\mu_B g_F m_F}{k_B} \Delta B(\mathbf{x}) = \frac{\mu_B g_F m_F}{k_B} \left[B_{max}^{i,l}(\mathbf{x}) - B_{min}^{i,l}(\mathbf{x}) \right] \quad (10)$$

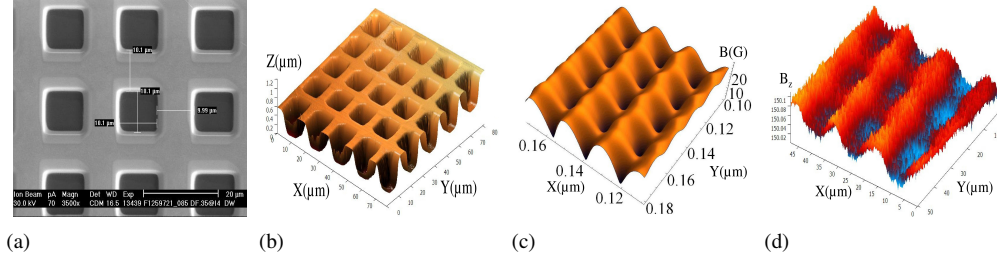


Fig. 4. (a) Scanning Electron Microscope (SEM) and (b) Atomic Force Microscope (AFM) images of the fabricated two-dimensional magnetic lattice. (c) Magnetic field minima B_{min}^z simulated across the surface of the magnetic lattice, where we simulate the application of in-situ bias field along the x -axis, $B_{x-bias} = 3$ G. (d) Magnetic Force Microscope (MFM) image showing the phase across the surface with the same conditions applied in the simulation.

where $\mathbf{x} = \{x, y, z\}$. The g_F is the Landé g -factor, μ_B is Bohr magneton, F is the atomic hyperfine state with the magnetic quantum number m_F and k_B is the Boltzmann constant. In Fig. 4, we show the measurement results for a fabricated 2×2 blocks of 9×9 asymmetric two-dimensional magnetic lattice. The quantum device is fabricated using the dual electron-focused ion beams technology and imaged with scanning electron microscope and the atomic force microscope, as shown in Figs. 4(a)–4(b). The structure is designed in such a way that allows in-situ magnetic field bias to be applied along the x -axis. The measurement output and the simulation results are shown in Figs. 4(c)–4(d).

3. Tunneling Mechanisms in the Two-Dimensional Magnetic Lattice

Experimentally, well spaced clouds of Bose-Einstein condensates in a double-well potential have been created [9], and a long tunneling lifetime of 50 ms has been observed [10] with experimental lifetimes in the range 1-100 s [11]. In this proposal, weakly coupled microscopic clouds of BECs, with a small number of trapped ultracold atoms, are allowed to tunnel between sites by adiabatically controlling the hopping strength of the adjacent magnetic bands through application of external magnetic bias fields along the negative direction of the z -axis. Atoms tunnel through the magnetic barriers from the highest magnetic band to the neighboring lowest magnetic band following the pyramid-like distribution of energy levels. Figures 2(b)–2(c) shows simulation results of two adjacent edge lattice sites where the gap can also be regarded as the difference between the heights of the two sites in the earth's gravitational fields.

In each individual site there are a number of available energy levels due to the magnetic field confinement and available degrees of quantum degeneracy. We consider in our scenario a two-level quantum system configuration in which there is a vibrational ground state $\phi_{i,j}^g$ and a vibrational excited state $\phi_{i,j}^e$ in each single lattice site at the i^{th} (or j^{th}) magnetic band, where $i \neq j \in \{1, \dots, n\}$ is the potential well index starting from the center site. The sites are characterized by a configured magnetic bottom B_{min} to trap alkali atoms which are magnetically prepared in a low magnetic field seeking state. Our system consists of n quantum wells (QWs) that are indirectly coupled via the magnetic band gap. In the asymmetrical QWs, we consider the two lowest energy state, in each individual potential well, i.e., an individual lattice site, are closely spaced and well separated from the other higher levels within the lattice site. This is a picture of a two-level quantum system with negligible interaction between the many bosons distributed in the two energy levels of the system, permitting the two-mode approximation of the many-body problem in our proposed magnetic lattice [9, 10, 13].

The general second-quantized Hamiltonian, in terms of bosonic creation, $\hat{\Phi}^\dagger(\mathbf{x})$, and annihilation, $\hat{\Phi}(\mathbf{x})$, field operators, for a system of N interacting boson of mass M confined by an external magnetic potential $B(\mathbf{x})$ at zero temperature is given by

$$\begin{aligned}\hat{H}_{\text{sys}} = & \int d\mathbf{x} \hat{\Phi}^\dagger(\mathbf{x}) \left(-\frac{\hbar^2}{2M} \nabla^2 + B(\mathbf{x}) \right) \hat{\Phi}(\mathbf{x}) \\ & + \frac{1}{2} \int d\mathbf{x} \hat{\Phi}^\dagger(\mathbf{x}) \left[\int d\mathbf{x}' \hat{\Phi}^\dagger(\mathbf{x}') U_{\text{int}}(\mathbf{x} - \mathbf{x}') \hat{\Phi}(\mathbf{x}') \right] \hat{\Phi}(\mathbf{x})\end{aligned}\quad (11)$$

The field operators obey the usual canonical commutation rules. The second term in this equation represents the many-bosons interaction in the usual zero-range approximation, where in the s -wave limit the inter-atomic potential reduces to $U_{\text{int}}(\mathbf{x} - \mathbf{x}') \rightarrow g = 4\pi\hbar^2 a_s / M$. The coupling constant g is determined from the scattering length a_s . For an $n \times n$ asymmetric magnetic lattice with n magnetic bands and no tunneling between sites, i.e., the case of uncoupled magnetic bands, the individual lattice site i of the two energy levels $k \in \{0, 1\}$ allows a localized single wave function of the condensate to be in the ground state, taking the form

$$\phi_i^{[k,m]}(\mathbf{x} - \mathbf{x}_i) = \langle \mathbf{x} | i, k, m \rangle \quad (12)$$

which can be approximated by the eigenfunction of an isotropic simple harmonic oscillator. The superscript m accounts for the quanta of angular momentum in the z -direction, where the value of the index m depends on the value of k such that for $k = 0$ there is no angular momentum, i.e., $m = 0$, and for $k = 1$, $m \in \{-1, 0, 1\}$ in the three dimensions [14, 15]. In the followings, we give a general description for the Hamiltonian and the state vectors in such away that it can also be used to describe a spinor Bose-Einstein condensate or ultracold fermions. In both scenarios the proposed magnetic lattice can be used to simulate Josephson oscillations and exciton as well as biexciton formation [26].

There are two modes in each individual lattice site. The lower mode, $\phi_i^{[0,m]}$, is essentially symmetric and the second mode, $\phi_i^{[1,m]}$, is antisymmetric. Due to the initially tilted n potential wells, the tunneling of the condensate produces a superposition between the higher magnetic band ground state mode $\phi_i^{[0,m]}$ and the adjacent lower band excited mode, $\phi_j^{[1,m]}$. The superposition amplitude strongly depends on the spatial separation of the wells determined by α_s where $\Delta B^i = B_{\text{max}}^i - B_{\text{min}}^i \approx \alpha^2 / 2$ [19]. Dynamically, interacting bosonic cold atoms in n potential wells with tight $B(\mathbf{x})$ magnetic field confinement can be described by generalizing, for n sites, the quantized Josephson or a two-mode Bose-Hubbard Hamiltonian, assuming the site number distribution starts from the center of the magnetic lattice

$$\begin{aligned}\hat{H}_{BH} = & - \sum_{j \neq i=1}^n J_{i,j}^{[k,m]} \left(\hat{\mathbf{b}}_i^\dagger \hat{\mathbf{b}}_j + \hat{\mathbf{b}}_j^\dagger \hat{\mathbf{b}}_i \right) + \sum_{j \neq i=1}^n \frac{U_{i,j}^{[k,m]}}{2} \left(\hat{\mathbf{n}}_i [\hat{\mathbf{n}}_i - 1] + \hat{\mathbf{n}}_j [\hat{\mathbf{n}}_j - 1] \right) + \\ & + \delta B \sum_{i \neq j} \left(\hat{\mathbf{b}}_i^{\dagger[k,m]} \hat{\mathbf{b}}_j^{[k',m]} + \hat{\mathbf{b}}_j^{\dagger[k',m]} \hat{\mathbf{b}}_i^{[k,m]} \right), \quad k \neq k' \in \{0, 1\}\end{aligned}\quad (13)$$

where $\hat{\mathbf{b}}_{i,j}^\dagger$ and $\hat{\mathbf{b}}_{i,j}$ are the bosonic creation and annihilation operators obeying the canonical commutation rules, and $\hat{\mathbf{n}}_{i,j} = \hat{\mathbf{b}}_{i,j}^\dagger \hat{\mathbf{b}}_{i,j}$ is the bosons number operator and δB is the tilting magnetic potential. The $J_{i,j}^{[k,m]}$ and $U_{i,j}^{[k,m]}$ are tunneling and inter-lattice site boson-boson interaction parameters, respectively, defined as

$$J_{i,j}^{[k,m]} = - \int d\mathbf{x} \phi_{i,j}^{*[k,m]}(\mathbf{x} - \mathbf{x}_i) \left(-\frac{\hbar^2}{2M} \nabla^2 + B(\mathbf{x}, t) \right) \phi_{i,j}^{[k,m]}(\mathbf{x} - \mathbf{x}_j) \quad (14)$$

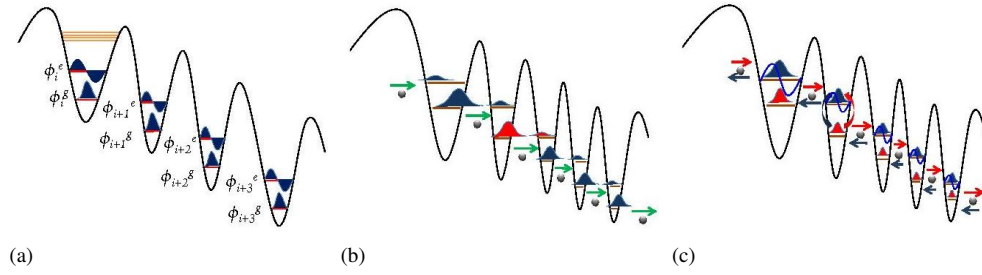


Fig. 5. (a) Schematic representation of the two-mode system ϕ_i^s, ϕ_i^e . (b-c) Representation of the Josephson oscillation, i.e., adiabatically induced Josephson current, and the coupling between two different states at each pair of adjacent sites, respectively. The schematic representation shows only one site of the propagating Josephson currents.

$$U_{i,j}^{[k,m]} = \frac{3g}{8} \int d\mathbf{x} |\phi_{i,j}^{[0,0]}(\mathbf{x} - \mathbf{x}_j)|^4 \quad (15)$$

When $\delta B = 0$, the Bose-Hubbard Hamiltonian describes the noninteracting magnetic bands where the condensate is assumed to occupy the ground state $\phi_{i,j}^{[0,0]}$ of an individual lattice site in each magnetic band with a single-mode one-level configuration regardless of the existence of the excited mode. This is because the no-tunneling condition results in inter-site many boson interaction which creates a lattice structure described in the Fock regime as will be explained in the following section. A typical characteristic that can be encountered in such a situation is the Mott insulator state [13, 27].

Since our interest is in the adiabatically induced transition process, we only summarize the case where the trapped ultracold atoms exhibit a superposition between the vibrational ground state $\phi_i^{[0,m]}$ in the QW_i and the vibrational excited state $\phi_j^{[1,m]}$ in the QW_j . This is a simultaneous bi-directional Josephson transition between each pair of adjacent magnetic bands propagating from the center towards the edges of the lattice, i.e. along x, y and $-x, -y$ directions, as schematically represented in Fig. 5(b).

Based on the configuration of this new type of magnetic lattice, we realize that the number of sites n creates interesting configurations at the center of the lattice. When n takes odd values, i.e., $n = 5, 7, 9, \dots$, there is only one center site screened by the surrounding four sites. In this case of a single center site, the induced tunneling interaction is dominated by the equivalent Coulomb potentials between the four surrounding sites distributed along the $x - y$ magnetic bands and taking a molecule-like configuration which can be created only in bound states assuming that there are symmetrical tunneling amplitude in the four directions. When n takes even values, i.e., $n = 4, 6, 8, \dots$, there are four symmetrical center sites which exhibit a first Brillouin zone dimensionality and hence have Bloch interacting wave functions and a field operator expanded in localized single-particle wave functions of the form

$$\hat{\Phi}(\mathbf{x}) = \sum_{i=1}^4 \hat{\mathbf{b}}_i^\gamma \phi_{1,\gamma}^{[k,m]}(\mathbf{x}) \quad (16)$$

where $\phi_{1,\gamma}^{[k,m]}$ represents the Bloch wave function with $k = 0$, and γ is the wave vector in the first Brillouin zone. $\hat{\mathbf{b}}_m^\gamma$ is the usual bosonic annihilation operator. The center tunneling mechanism

allows the Bloch wave function $\phi_{1,\gamma}^{[k,m]}$ via the standard eigenvalue problem

$$\left(-\frac{\hbar^2}{2m} \nabla^2 + \Delta B(\mathbf{x}) \right) \phi_{1,\gamma}^{[k,m]} = E_{1,\gamma} \phi_{1,\gamma}^{[k,m]} \quad (17)$$

This situation is similar to the band structure in a two-dimensional optical lattice; however, in our asymmetric two-dimensional magnetic lattice, it is limited to the four center sites when n is even [8]. This is because there is no tilting potential between the four sites, $\delta B = 0$. When the tunneling is allowed between the four sites only the excited states, $\phi_1^{[1,m]}$ contribute to the local tunneling amplitude between the four sites where the superposition state is described for the four center sites $\{a, b, c, d\}$ via the coupling amplitude such that $J_1^{[1,m]} \left[\phi_{1,a}^{[1,m]} \phi_{1,b}^{*[1,m]} + \phi_{1,b}^{[1,m]} \phi_{1,c}^{*[1,m]} + \phi_{1,c}^{[1,m]} \phi_{1,d}^{*[1,m]} + \phi_{1,d}^{[1,m]} \phi_{1,a}^{*[1,m]} \right]$.

The vibrational ground states, $\phi_1^{[0,m]}$ contribute to the interaction mechanisms between the four center sites and the sites of the surrounding first magnetic band where the local interaction of the excited mode, $\phi_1^{[1,m]}$, between the four sites is assumed to be negligible. As will be described in the following section, this picture can be generalized to describe, regardless of the asymmetrical feature, the Mott insulator quantum phase transition across the $n \times n$ two-dimensional magnetic lattice via the discharging Josephson state. The quantum phase transition can be oscillating adiabatically, a significant feature for quantum information processing in such type of magnetic lattices.

4. Josephson Oscillations and the Excitons Mott Phase Transition

The two well known regimes, the Josephson regime and the Fock regime, can be applied to our approach to describe the outcome of the tunneling process of the trapped ultracold atoms [16]. Regardless of the asymmetrical effect in our two-dimensional magnetic lattice, one can still describe the transitions between the lattice sites as an induced Josephson current, i.e., the superfluid phase transition, between two recognizable states which are the Mott insulator state and the discharging Josephson state in which the adiabatically controlled Josephson current oscillation depends on the coupling values. We describe briefly in the following the required conditions for such transitions.

• Mott Insulator State

In the non-interacting regime where the first-mode $\phi_{i,j}^{[0,m]}$ is regarded as the ground state and as a solution for the Schrödinger equation with negligible inter-site interactions regardless of the existence of the excited mode $\phi_{i,j}^{[1,m]}$, the condensate is said to have an individual mode solution of the form $\phi_{i,j}^g = \phi_{i,j}^{[0,m]}(\mathbf{x} - \hat{\mathbf{x}})$ [19]. Initially, there is an approximately equal number of atoms in each site $N_s \approx N/n$, where this number is fixed until tunneling is allowed. The atoms are completely localized at the lattice site where we assume the coupling strength between the two levels is very weak such that

$$N_s |U_{i,j}^{[0,0]}| \ll \Delta E_{i,j}^{[k,m]} = 2 \left[E_{i,j}^{[1,m]} - E_{i,j}^{[0,m]} \right] = \hbar \omega \quad (18)$$

where $\Delta E_{i,j}^{[k,m]}$ is the energy difference. Localization in our scenario means that the first symmetric mode, $\phi_{i,j}^g$, is dominating over all lattice sites and the expansion of the excited mode, $\phi_{i,j}^e$, between each two adjacent magnetic bands is negligible. This condition can be thought

of as the Fock regime where the on-site interaction is greater than the hopping strength, $U_i^{[0,m]} \leftrightarrow U_i^{[1,m]} \gg J_{i \leftrightarrow j}^{[0 \rightarrow 1,m]}$. It is a signature of the Mott insulator state where all particles are localized in the ground state, neglecting the excited level, with a defined number of atoms at each site exhibiting no coherence nor a macroscopic wave function and permitting a one-level approximation having a one-level Bose-Hubbard Hamiltonian for the $n \times n$ asymmetric magnetic lattice of the form

$$\hat{H}_{1HB} = - \sum_{j \neq i=1}^n J_{i,j}^{[0,0]} \left(\hat{\mathbf{b}}_i^\dagger \hat{\mathbf{b}}_j + \hat{\mathbf{b}}_j^\dagger \hat{\mathbf{b}}_i \right) + \sum_{j \neq i=1}^n \frac{U_{i,j}^{[0,0]}}{2} \left(\hat{\mathbf{n}}_i [\hat{\mathbf{n}}_i - 1] + \hat{\mathbf{n}}_j [\hat{\mathbf{n}}_j - 1] \right) \quad (19)$$

where $\delta B = 0$, and \hat{H}_{1HB} describes a finite number of sites. In the case of an infinite number of sites, Eq. (18) describes the single-band Bose-Hubbard Hamiltonian for weakly interacting bosons in a symmetric magnetic lattice, i.e., $\hat{H}_{1HB} \rightarrow \hat{H}_{HB}$. Note that the operators $\hat{\mathbf{b}}_{i,j}^\dagger, \hat{\mathbf{b}}_{i,j}$ and $\hat{\mathbf{n}}_{i,j}$ are for the case of $k = m = 0$. The Fock space state vector takes the form

$$|\varphi\rangle = \sum_{n_{i,j}=0}^{N+1} c_{i,j}^{[0,0]} |\mathbf{n}_i, \mathbf{n}_j\rangle \quad (20)$$

Here the size of the Hilbert space is roughly estimated to be $(N+1)$ and $c_{i,j}^{[0,0]}$ represents the ground state amplitude.

• Exciton Mott Quantum Phase Transition via the Induced Josephson Atomic Current

The situation where the hopping strength is increased adiabatically, can typically be described using the self-consistent nonlinear Schrödinger equation, i.e., the Gross-Pitaevskii equation (GPE)

$$i\hbar \frac{\partial \varphi_i(\mathbf{x}, t)}{\partial t} = \left[-\frac{\hbar^2}{2m} \nabla^2 + B(\mathbf{x}) + g \|\varphi_i(\mathbf{x}, t)\|^2 \right] \varphi_i(\mathbf{x}, t) \quad (21)$$

which represents the nonlinear generalization of the sinusoidal Josephson oscillations occurring in superconducting junctions, described in some detail in [17, 18, 28]. It also allows the notion of the generalized tunneling mechanisms of the condensate between two sites to be applied to the n asymmetric magnetic bands where the field operator is expanded in terms of the static ground state solution, ϕ_i^g , of the GPE Eq. (21) for each individual uncoupled lattice site, and in terms of the amplitude of the relative population $N_i^s \equiv N_i^s$ expressed as $\psi_i(\mathbf{x}, t) = \sqrt{N_i^s(\mathbf{x}, t)} e^{i\theta_i(t)}$, where θ_i is the corresponding phase [29]. Thus we expand the field operator as

$$\varphi_i(\mathbf{x}, t) = \sqrt{N} \sum_{i=1}^n \psi_i(\mathbf{x}, t) \phi_i^g \quad (22)$$

Hence the evolution of the ultracold atoms population $N_i^s(t)$ of the n sites can be obtained by integrating the spatial distributions $\varphi_i(\mathbf{x}, t)$ to obtain the time dependent equation [16, 18, 29]

$$i\hbar \frac{\partial \psi_i(\mathbf{x}, t)}{\partial t} = \left[\Omega_{i,j}(\mathbf{x}, t) + U_{i,j}^{[0,m]} N |\psi_i|^2 \right] \psi_i - \sum_{i \neq j}^n J_{i,j}^{[0,m]}(\mathbf{x}, t) \psi_j \quad (23)$$

where

$$\Omega_{i,j}(\mathbf{x}, t) = \int d\mathbf{x} \left[\frac{\hbar^2}{2M} |\nabla \phi_i^{*g}|^2 + \phi_i^{*g} B(\mathbf{x}, t) \phi_i^g \right] \quad (24)$$

Equation (23) is known as the Bose Josephson junction (BJJ) tunneling equation which can be re-derived in terms of the phase differences and the fractional population differences between the lattice n sites. A similar case of a double well is discussed in [19]. The transition from self-trapping to Josephson oscillating states [10, 12] is possible in this type of asymmetrical magnetic lattice having several uncoupled magnetic bands which can be coupled via the induced Josephson current or it can be described as a Josephson discharging state created via quantum cold collisions.

Starting from the Mott insulator state and by adiabatically tuning the hopping strength via the application of $B_{-z-bias}$, the number of atoms in each site N_s varies in time to a critical number of atoms that is periodically oscillating and predicted to produce the n magnetic inter-band Josephson oscillations. Schematic representations are shown in Fig. 5. The quantum state of the asymmetrical magnetic lattice at this point of the transition belongs to what is known as the Josephson regime, where the in-site (inter-well) many boson interaction of the two energy states $k = 0$ and $k = 1$ is very small compared to the off-site many boson interaction, namely the condition

$$U_i^{[0,m]} \leftrightarrow U_i^{[1,m]} \ll J_{i \leftrightarrow j}^{[0 \rightarrow 1,m]} \quad (25)$$

The dominant transition at the critical number of atoms is, starting from the center of the lattice, the n magnetic band one-directional Josephson transition, $\phi_i^{[0,m]} \rightarrow \phi_j^{[1,m]}$. Oscillating bound states will be created in both situations, on and off-sites leading to exciton Mott multi-transitions. The on-site bound state is created between the ground state and the excited state, e.g., two different components of a spinor BEC trapped in a single site. This is due to the dipole interaction which occurs when the condensate in the excited state periodically couples to the oscillating ground state at each individual site. The number of atoms may play an important role in such a scenario where it might be required to have an equal number of atoms in both modes [20–22]. The fragmented condensate in the ground state of each site couples periodically via the Coulomb potential to the excited state in the neighboring site exhibiting a recombination rate between two different adjacent magnetic bands with a plasma oscillation frequency relative to the strength of the Coulomb interaction which is experimentally realized in a single bosonic Josephson junction [10]. This can also be thought of as a difference in the chemical potential between sites in the case of trapped ultracold fermions.

5. Conclusion

We have developed a new method to create an asymmetric two-dimensional magnetic lattice. In this article we have proposed one of the applications that can be realized using this type of quantum device, where trapped ultracold atoms can simulate the critical quantum phase transition of collective excitations such as the exciton-Mott bound states and the oscillation mechanisms of the Mott insulator to a discharging Josephson state. In our approach, adiabatically controlled coherent tunneling of the ultracold atoms will induce a dc and ac Josephson current, a significant feature that can be used to encode and transfer, across the 2D asymmetrical lattice with $n \times n$ Josephson qubits for quantum information processing. We have established a theoretical framework that can be used to calculate the relevant parameters required to describe the fundamental concepts.

Acknowledgment

We thank James Wang, from the Centre for Atom Optics and Ultrafast Spectroscopy in Swinburne University, for performing the atomic force microscope and magnetic force microscope measurements.